MOLECULAR AND CELLULAR BIOLOGY, June 2011, p. 2276–2286 Vol. 31, No. 11
0270-7306/11/$12.00 doi:10.1128/MCB.01105-10

Lack of Protein 4.1G Causes Altered Expression and Localization of the Cell Adhesion Molecule Nectin-Like 4 in Testis and Can Cause Male Infertility▽

Shaomin Yang,[1,4] Haibo Weng,[1] Lixiang Chen,[1] Xinhua Guo,[1] Marilyn Parra,[1] John Conboy,[5] Gargi Debnath,[1] Amy J. Lambert,[3] Luanne L. Peters,[3] Anthony J. Baines,[6] Narla Mohandas,[1] and Xiuli An[1,2]*

Red Cell Physiology Laboratory,[1] Laboratory of Membrane Biology,[2] and Mammalian Genetics Laboratory,[3] New York Blood Center, New York, New York 10065; Department of Pathology, Peking University Health Science Center, Beijing 100191, China[4]; Life Science Division, Lawrence Berkeley National Laboratory, Berkeley, California 94720[5]; and School of Biosciences, University of Kent, Canterbury, Kent CT2 7NJ, United Kingdom[6]

Received 21 September 2010/Returned for modification 19 November 2010/Accepted 22 March 2011

Protein 4.1G is a member of the protein 4.1 family, which in general serves as adaptors linking transmembrane proteins to the cytoskeleton. 4.1G is thought to be widely expressed in many cells and tissues, but its function remains largely unknown. To explore the function of 4.1G *in vivo*, we generated 4.1G$^{-/-}$ mice and bred the mice in two backgrounds: C57BL/6 (B6) and 129/Sv (129) hybrids (B6-129) and inbred B6. Although the B6 4.1G$^{-/-}$ mice showed no obvious abnormalities, deficiency of 4.1G in B6-129 hybrids was associated with male infertility. Histological examinations of these 4.1G$^{-/-}$ mice revealed atrophy, impaired cell-cell contact and sloughing off of spermatogenic cells in seminiferous epithelium, and lack of mature spermatids in the epididymis. Ultrastructural examination revealed enlarged intercellular spaces between spermatogenic and Sertoli cells as well as the spermatid deformities. At the molecular level, 4.1G is associated with the nectin-like 4 (NECL4) adhesion molecule. Importantly, the expression of NECL4 was decreased, and the localization of NECL4 was altered in 4.1G$^{-/-}$ testis. Thus, our findings imply that 4.1G plays a role in spermatogenesis by mediating cell-cell adhesion between spermatogenic and Sertoli cells through its interaction with NECL4 on Sertoli cells. Additionally, the finding that infertility is present in B6-129 but not on the B6 background suggests the presence of a major modifier gene(s) that influences 4.1G function and is associated with male infertility.

Protein 4.1G is a member of the protein 4.1 family, which includes four members: 4.1R (9), 4.1G (31), 4.1B (30), and 4.1N (48). These molecules share high sequence homology in three functional domains: the N-terminal 4.1-ezrin-radixin-moesin (FERM) domain, the internal spectrin-actin binding domain (SABD), and the C-terminal domain (CTD). The prototypical member of the family, 4.1R, was first discovered in erythrocytes, where it plays a critical role in maintaining the shape and mechanical stability of the cell membrane (37, 44). In addition, 4.1R has been shown to play diverse roles in many nonerythroid cells (10, 16–18, 52).

In contrast to 4.1R, very little is known about the function of 4.1G. Earlier *in situ* hybridization and mRNA dot blot analysis suggested that 4.1G mRNA is generally distributed in all tissues (30). More recently, real-time PCR analysis revealed that 4.1G is predominately expressed in brain, spinal cord, and testis (42). It has been reported that, in mouse testis, 4.1G is expressed along the membrane of Sertoli cells and may be involved in the adhesion between Sertoli cells and spermatogenic cells (46). However, the physiological role of 4.1G in testis has yet to be fully identified.

In mammals, the functional unit of the testis is the seminiferous tubule, where spermatogenesis occurs. During this process, spermatogonia go through three sequential, distinct cellular and molecular phases (mitosis, meiotic phase, and spermiogenesis) to differentiate into fully developed spermatids (spermatozoa). Throughout spermatogenesis, all developing germ cells are in direct contact with Sertoli cells for structural and nutritional support (8). Thus, the adhesion between Sertoli cell and germ cell plays a critical role in spermatogenesis. It has been shown that the adhesion defects between Sertoli cells and germ cells lead to male infertility (1, 15).

To elucidate the physiological function of 4.1G *in vivo*, we generated 4.1G knockout mice. We found that lack of 4.1G led to male infertility in C57BL/6 (B6) and 129/Sv (129) hybrid (B6-129) mice but not in B6 inbred mice. We further showed the decreased expression and altered localization of the nectin-like 4 (NECL4) adhesion molecule in 4.1G$^{-/-}$ testis, which is accompanied by impaired cell-cell contact. These findings suggest that 4.1G mediates cell-cell contact between Sertoli cells and germ cells through its interaction with NECL4 on Sertoli cells.

MATERIALS AND METHODS

Generation and use of 4.1G knockout mice. Embryonic stem (ES) cells containing a gene trap cassette inserted downstream of 4.1G exon 2 were obtained from the Sanger Institute Gene Trap Resource (SIGTR; ES cell line AL0682). The gene trap insertion site was confirmed by reverse transcriptase PCR (RT-

* Corresponding author. Mailing address: Laboratory of Membrane Biology, 310 E 67th St., New York, NY 10065. Phone: (212) 570-3247. Fax: (212) 570-3264. E-mail: xan@nybloodcenter.org.

▽ Published ahead of print on 11 April 2011.

PCR) to validate splicing of the cassette to 4.1G exon 2. ES cells were microinjected into blastocysts and implanted into recipient female mice to permit development of the embryos into chimeras at the University of California, San Francisco, transgenic facility, and subsequent breeding was performed to select founders with germ line transmission of the gene trap allele. Primer set β-geoFOR (GTGGAAGTCTAGGTTTTCTTGTTGT) and β-geoREV (CTCGGCTGAGGACTCCCT) was used to determine the cassette insertion, and the primer set 4.1GFOR (TGTGTGTGGTTTGCTTGTGGAAGTC) and 4.1GREV (ATCTTGGGTATCCTAAGTTTCTGGGC) was used to detect the 4.1G gene. The mice were maintained on both a B6-129 hybrid background (in which the knockout mice were generated) and a congenic B6 background (backcrossed for 9 generations). The mice were initially bred and screened at the Lawrence Berkeley National Laboratory (LBNL) animal facility and then maintained at the animal facility of New York Blood Center under specific-pathogen-free conditions according to institutional guidelines. Animal protocols were reviewed and approved by the Institutional Animal Care and Use Committees at both institutions.

Antibodies. Rabbit polyclonal anti-β-catenin and anti-GAPDH (glyceraldehyde-3-phosphate dehydrogenase) antibodies were purchased from eBioscience and Sigma-Aldrich, respectively. A polyclonal guinea pig anti-NECL4 antibody was kindly provided by James Salzer (New York University). The anti-NECL4 antibody used for immunoprecipitation experiment was from Abcam (Cambridge, MA). Polyclonal anti-4.1 antibodies were raised in rabbit and have been described in our previous study (17).

Immunoblot analysis. Total protein from tissues was prepared as follows: adult mice were sacrificed and the organs rapidly removed and sonicated in ice-cold buffer containing 0.32 M sucrose, 0.01 M HEPES (pH 7.4), 2 mM EDTA, 1 mM dithiothreitol (DTT), and protease inhibitor cocktail (Sigma-Aldrich, St. Louis, MO). The homogenate was spun at 900 × *g* for 5 min, and the supernatant was collected. Twenty micrograms of total protein was separated on an 8% SDS-PAGE gel and transferred to nitrocellulose membrane (Bio-Rad, Hercules, CA). The membranes were probed with rabbit anti-4.1G U1 (1:10,000), anti-4.1N U1 (1:1,000), anti-4.1B U1 (1:2,000), anti-4.1R exon 13 (1:1,000), guinea pig anti-NECL4 (1:1,000), rabbit anti-β-catenin (1:2,000), or rabbit anti-GAPDH (1:200,000) antibodies, followed by horseradish peroxidase (HRP)-conjugated goat anti-rabbit or anti-guinea pig IgG (Jackson Immuno Research, West Grove, PA). The films were developed using a Renaissance chemiluminescence detection kit (Pierce, Rockford, IL).

RT-PCR and amplification of testis 4.1G full-length cDNAs. Total RNA was prepared from testis using the RNeasy minikit (Qiagen, MD) and was reverse transcribed using the Superscript first-strand kit (Invitrogen, Carlsbad, CA) according to the manufacturer's instructions. Amplification of 4.1G transcripts was carried out using 2 μl of the first-strand cDNA and the 4.1G gene-specific primer set: 4.1GFOR (ATGACTACTGAAGTTGGCTCTGCATCTGAAGTG) and 4.1GREV (TTATTCTTCTCCTTCCTCCGCCAACTCTG) (49). PCR was performed in a 50-μl reaction mixture containing 10× PCR buffer, 10 μM primer mix, 2 μl RT product, and 1 μl of AccuPrime *Taq* DNA polymerase (Invitrogen, Carlsbad, CA). Cycling conditions were 30 s at 94°C, 30 s at 57°C, and 3 min at 68°C, followed by a final extension for 7 min at 72°C. Following 35 cycles, the resulting PCR products cloned into PCR 2.1-TOPO Vector (Invitrogen, Carlsbad, CA) were sequenced at the Memorial Sloan-Kettering Cancer Center (MSKCC) DNA Sequencing Core Facility.

To establish the exon organization and alternative splice sites of the variants, we compared the 4.1G (GenBank accession number AF044312) cDNA sequences with the genomic sequence using EST2GENOME in the EMBOSS suite (32) and exon composition displayed in Artemis (35).

Real-time quantitative PCR. Details meeting MIQE (minimal information for publication of real-time quantitative PCR [qPCR] experiments) (5, 6, 13) standards are provided to facilitate interpretation and reproducibility of results.

(i) RNA extraction. RNA was extracted using the TRIzol reagent lysis method of the PureLink RNA minikit and purified with PureLink DNase according to the manufacturer's directions (Invitrogen, Carlsbad, CA). Sample integrity and concentration were determined using the Agilent Bioanalyzer (Agilent Technologies Inc., Santa Clara, CA) and NanoDrop (NanoDrop Technologies, Wilmington, DE), respectively. All RNA integrity numbers (RIN) ranged between 9.0 and 10.0. Samples were stored at −80°C.

(ii) Reverse transcription. Total RNA (1 μg) was reverse transcribed using RETROscript random decamers (Ambion, Austin, TX) and SuperScript II (Invitrogen) according to the manufacturers' directions. Reactions for each sample were performed in triplicate on an MJ Research PTC 200 Peltier thermal cycler. The pooled reactions were tested for inhibitors by using both dilution curve and SPUD assay methods (28, 29).

(iii) qPCR. Reactions were performed on three biological samples per mouse strain using Power SYBR green (Applied Biosystems, Foster City, CA) master mix with 5 μl of 1:100 dilution of cDNA obtained from RT reactions and 1 μl of primer pairs in 20-μl reaction mixtures. The primer pair (FOR [GTTACTTCTGCCAGCTCTACAC] and REV [TCTCGGACCTCCACCACAG]) for NECL4 was designed and provided by PrimerDesign Ltd. (http://www.primerdesign.co.uk). A single peak was seen in the melt curve, indicating desired primer specificity. Biological samples were run in triplicate on an AB ViiA 7 real-time PCR system (Applied Biosystems, Foster City, CA). Cycle conditions consisted of 50°C for 2 min and 95°C for 10 min followed by 40 cycles of 95°C for 15 s and 60°C for 1 min. Each sample was tested with a no-template control and a no-reverse-transcriptase control.

(iv) Data analysis. Fluorescence data were collected by AB ViiA 7 real-time PCR system software (Applied Biosystems, Foster City, CA). Rn (normalized reporter signal) values were exported to LinRegPCR software (version 11.3, March 2009) for baseline and quantification cycle (Cq) determinations and to obtain amplicon group reaction efficiencies (33). Cqs and reaction efficiencies were exported to qBasePlus (version 1.4) to obtain relative normalized quantity (RQN) values (14). Three reference genes, *actb*, *B2M*, and *gapdh*, were also run.

Histology. Mice were anesthetized with pentobarbital and perfused via the heart with 10 ml 4% paraformaldehyde (PFA) in phosphate-buffered saline (PBS) (pH 7.4) to fix tissues *in vivo*. The testis and epididymis were removed immediately, fixed in Bouin's solution (Sigma-Aldrich, St. Louis, MO), and embedded in paraffin. Four-microliter-thick sections were processed for hematoxylin and eosin (H&E) staining. The testis sections were also stained with periodic acid-Schiff (PAS) (Diagnostic BioSystems, Pleasanton, CA), following the instructions by the manufacturer, to visualize the shape of the nucleus and acrosome to identify the stage of spermatid development. The stage of each seminiferous tubule was determined following the criteria described previously (34).

Immunohistochemistry. Paraffin-embedded testis sections (4 μm) were dewaxed in xylene and rehydrated in descending concentrations of ethanol. Antigen retrieval was achieved by boiling the sections in 10 mM citrate buffer for 20 min. Sections were stained with anti-4.1G U1 antibody (1:100) at room temperature for 1 h. After thorough washing with TBS-T (0.05 M Tris [pH 7.4], 0.15 M NaCl, 0.1% Tween 20), the sections were stained with HRP-conjugated secondary antibodies (DakoCytomation, Inc., Fort Collins, CO) for 40 min at room temperature and developed with the liquid DAB+ (diaminobenzidine) substrate chromogen system (DakoCytomation, Inc.). The nucleus was counterstained with hematoxylin (DakoCytomation, Inc.), and images were acquired with a Leica DM 2000 microscope (Leica Microsystems, Inc., Bannockburn, IL).

Separated testis cell smear preparation. The separated testis cells were prepared according to previously described methods (3) with minor modifications. Briefly, two decapsulated testes were digested with 0.5 mg/ml collagenase (Sigma-Aldrich) in Hanks solution, pH 7.4, with shaking at 34°C for 15 min to eliminate the interstitial cells, and then washed 3 times with PBS. To separate the Sertoli cells and germ cells, the testis tubules were further incubated in a mixture of enzymes containing 0.1% collagenase, 0.2% hyaluronidase (Sigma-Aldrich), 0.04% DNase I (Sigma-Aldrich), and 0.03% trypsin inhibitor (Sigma-Aldrich) in Hanks solution with shaking at 34°C for 40 min. After centrifugation, the cell pellet was collected and resuspended in Hanks solution and then filtered through 53-μm nylon mesh. The filtered cell drops were smeared on slides and dried in the hood. The H&E staining was performed as described above.

Electron microscopy. The mice were perfused with 4% glutaraldehyde in PBS, pH 7.4. The testis was removed, and small pieces of tissue were fixed in the same buffer for 4 h at 4°C. After being washed with PBS, tissues were postfixed in 1% osmium tetroxide (Electron Microscopy Science). The samples were dehydrated and embedded in epoxy resin. Ultrathin sections were cut onto copper grids, stained with uranyl acetate and lead citrate, and then observed using a Philips-410 transmission electron microscope (Philips, Eindhoven, Netherlands).

Immunofluorescence. For immunofluorescence staining of testis tissue, mice were perfused with 4% PFA as described above, and the testes were dissected and embedded in optimal cutting compound (OCT) (Sakura Finetek U.S.A.) and snap-frozen in liquid nitrogen. Cryosections (6 μm) were prepared, treated with 4% PFA and 0.1% Triton X-100 for 20 min at room temperature, and blocked with 10% horse serum and 1% bovine serum albumin (BSA) for 1 h at room temperature. The sections were incubated overnight at 4°C with guinea pig-derived anti-NECL4 antibody (1:100), followed by Alexa 488-conjugated donkey anti-guinea pig IgGs (Molecular Probes, Carlsbad, CA). After blocking again, the rabbit anti-4.1G antibody (1:100) and Alexa 594-conjugated donkey anti-rabbit IgGs (Molecular Probes, Carlsbad, CA) were applied in sequence. Sections were observed with a Nikon Eclipse E600 epifluorescence microscope (Nikon Inc., Japan). For immunofluorescence staining of separated testis cells, the smear was prepared as described above. After fixation and permeation with

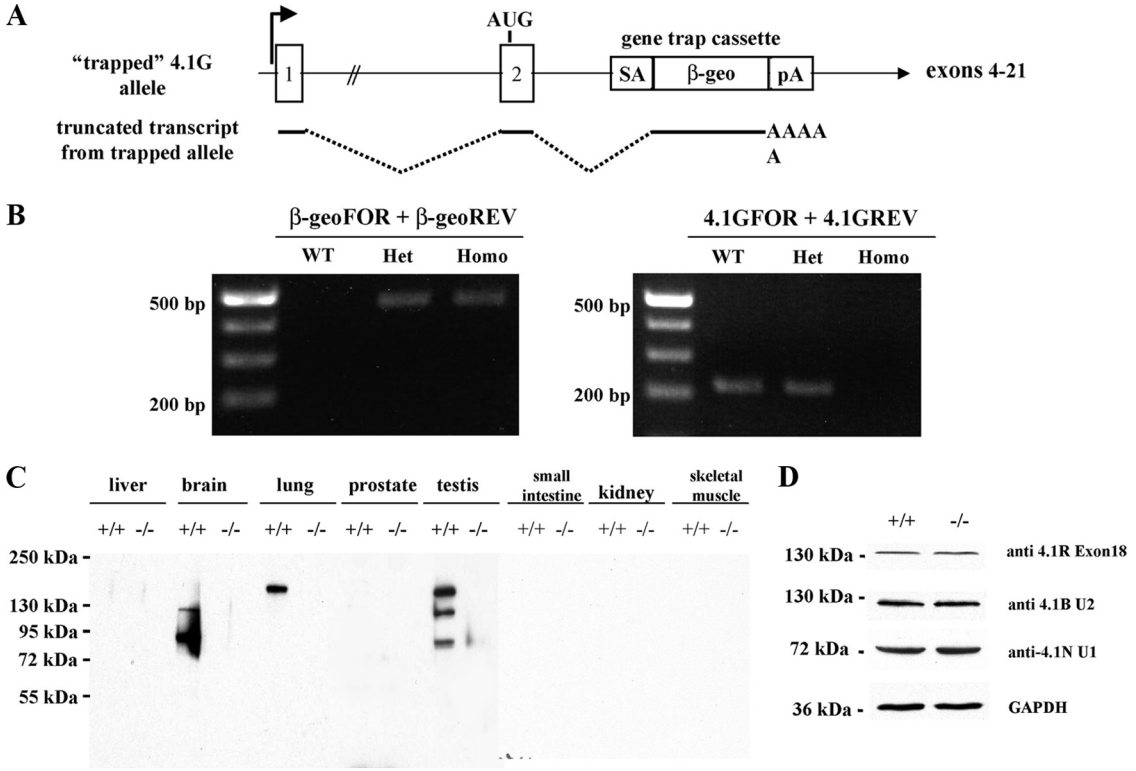

FIG. 1. Disruption of 4.1G gene expression. (A) Knockout strategy. An ES cell line containing the β-geo gene trap cassette inserted into intron 2 of the 4.1G gene was used to generate 4.1G-deficient mice. (B) Genotyping. Offsprings of heterozygous mating pairs were screened by PCR using primers that distinguish gene trap-targeted alleles and the wild type. Note that a 447-bp band was amplified by β-geo forward and reverse primers from heterozygous (Het) and homozygous (Homo) but not from wild-type (WT) mice. In contrast, a 229-bp band was amplified by 4.1G forward and reverse primers from WT and heterozygous but not homozygous mice. (C) Western blot analysis. Note the expression of 4.1G isoforms in $4.1G^{+/+}$ brain, lung, and testis but not in liver, prostate, small intestine, kidney, and skeletal muscle under the same experimental conditions. No 4.1G protein expression was detected in tissues of the $4.1G^{-/-}$ mice. (D) Western blot analysis of other members of the protein 4.1 family in testis. Lysate (20 μg) from $4.1G^{+/+}$ or $4.1G^{-/-}$ testis was subjected to immunoblot analysis with polyclonal rabbit antibodies against 4.1R exon 18, 4.1B U1, 4.1N U1, and GAPDH. No difference was observed in the expression levels of 4.1R, 4.1B, and 4.1N in $4.1G^{+/+}$ and $4.1G^{-/-}$ testis.

4% PFA and 0.1% Triton X-100 for 20 min at room temperature, the cell smears were blocked with 10% horse serum and 1% BSA for 1 h at room temperature. Then the slides were incubated with rabbit anti-4.1G U1 antibody (1:100) at 37°C for 1 h, Alexa 488-conjugated donkey anti-rabbit IgGs (1:600) at 37°C for 30 min, and 1 U Texas Red-X phalloidin (Molecular Probes, Carlsbad, CA) at room temperature for 40 min, in sequence. After being washed three times with PBS, the slides were mounted in fluorescence mounting medium containing DAPI (4′,6-diamidino-2-phenylindole) (Vector Labs, Burlingame, CA) and observed with a Nikon Eclipse E600 fluorescence microscope.

Coimmunoprecipitation. Two testes from wild-type (WT) mice were lysed in ice-cold radioimmunoprecipitation assay (RIPA) buffer (Millipore, Billerica, MA) with 10% protease inhibitor cocktail for 30 min. After centrifugation at 16,000 × *g* at 4°C for 10 min, the supernatant was collected and protein concentration measured by the Bradford method using BSA as the standard. One milligram of extract was incubated with 5 μg rabbit anti-4.1G headpiece antibody, anti-NECL4 antibody, or preimmune IgG in 500 μl of the above-mentioned buffer at 4°C overnight with constant mixing and subsequently incubated with magnetic protein G agarose beads (Millipore, Billerica, MA) at 4°C for 1 h. The immunoprecipitate was isolated from immobilized protein G beads and separated by 10% SDS-PAGE followed by transfer to nitrocellulose membrane. The membrane was probed with rabbit anti-4.1G headpiece antibody and rabbit anti-NECL4 antibody (Abcam, Cambridge, MA).

cDNAs for recombinant proteins. His-tagged full-length 4.1G in pET30a(+) vector and the glutathione *S*-transferase (GST)-tagged cytoplasmic domain of NECL4 in pGEX-4T-3 vector were kindly provided by Philippe Gascard (UCSF) and James Salzer (New York University), respectively. GST-tagged 4.1G domains were subcloned into pGEX-4T-2 using BamHI and SalI upstream and downstream, respectively. Maltose binding protein (MBP)-tagged cytoplasmic domain of NECL4 was cloned into pMAL-c2X using BamHI and SalI restriction enzymes; the GST-tagged cytoplasmic domain of NECL4 in pGEX-4T-3 served as the template. The fidelity of all the constructs was confirmed by DNA sequencing.

Preparation of recombinant proteins. The plasmid DNA encoding various recombinant proteins was transformed into *Escherichia coli* BL21(DE3) for protein expression. The recombinant proteins were expressed at 16°C in the presence of 0.1 mM isopropyl-β-D-thiogalactopyranoside (IPTG). His-tagged 4.1G isoforms were purified by a nickel column, GST-tagged 4.1G domains were purified by a glutathione Sepharose 4B affinity column, and the MBP-tagged cytoplasmic domain of NECL4 was purified by amylose resin.

Pulldown assays. To examine the binding of full-length 4.1G to NECL4, the GST-tagged cytoplasmic domain of NECL4 or GST alone was coupled to glutathione Sepharose 4B beads at room temperature for 30 min. Beads were pelleted and washed. His-tagged full-length 4.1G was added to the beads in a total volume of 100 μl. The final concentrations of both coupled protein and the protein in solution were 1 μM. The mixture was incubated for 1 h at room temperature, pelleted, washed, and eluted with 10% SDS. Protein brought down was detected by Western blotting using anti-4.1G antibody. To examine the interaction of various domains of 4.1G with the cytoplasmic domain of NECL4, GST-tagged recombinant proteins representing different 4.1G domains were coupled to glutathione Sepharose 4B beads, and the MBP-tagged cytoplasmic domain of NECL4 was added to the beads in a total volume of 100 μl. The binding assay was performed as described above, and the binding was detected by Western blotting using anti-MBP antibody.

RESULTS

Generation of $4.1G^{-/-}$ mice. To explore the function of 4.1G *in vivo*, we generated $4.1G^{-/-}$ mice using ES cells obtained

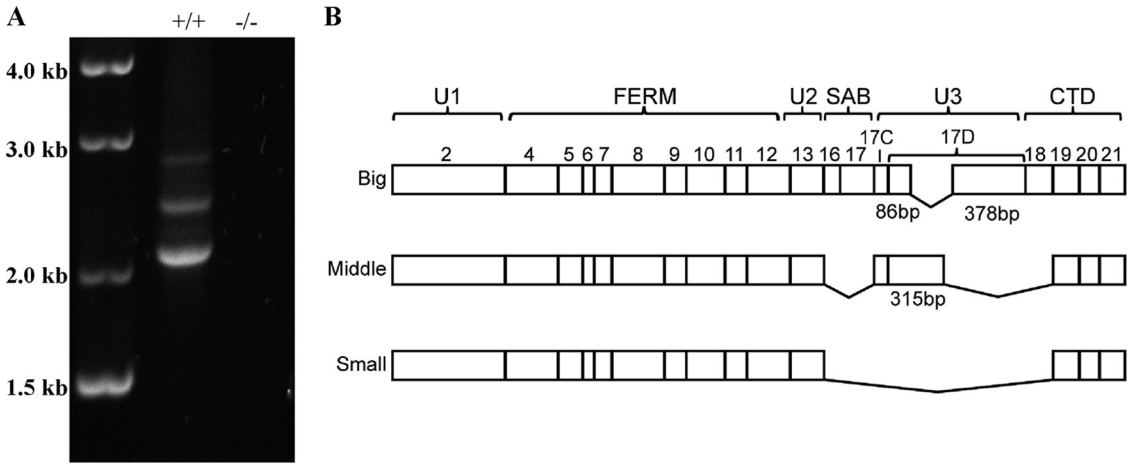

FIG. 2. Characterization of testis 4.1G. (A) Amplification of 4.1G transcripts from mouse testis. The 4.1G transcripts were amplified as described in Materials and Methods. Sizes of DNA ladders are indicated. (B) Schematic presentation of protein structure and exonic maps of mouse testis 4.1G isoforms.

from the Sanger Institute Gene Trap Resource, in which 4.1G expression was abrogated by insertion of a gene trap cassette that splices to exon 2 and terminates transcription prematurely (Fig. 1A). Genotyping results, using the primer set for the β-geo cassette or 4.1G gene, are shown in Fig. 1B, and they reveal that the primer set for the β-geo cassette amplified a 447-bp band from heterozygous and homozygous but not from wild-type mice. In contrast, the 4.1G forward and reverse primer set amplified a 229-bp band from WT and heterozygous but not homozygous mice. These results demonstrate the insertion of the β-geo cassette and the abrogation of the 4.1G gene expression. The targeted 4.1G allele could theoretically encode part of the N-terminal headpiece of the protein, but no such fragments were detected by Western blot analysis with anti-headpiece antibody (Fig. 1C). Figure 1C further shows that isoforms of 4.1G were observed as prominent bands in normal brain, lung, and testis but not in the same tissues of $4.1G^{-/-}$ mice. These data confirm that the gene trap cassette has resulted in a functional knockout of 4.1G. The detection of multiple bands in testis and brain indicates the presence of differentially spliced isoforms as described previously (43). No 4.1G protein was detected in liver, prostate, small intestine, kidney, and skeletal muscle under the same experimental conditions. In addition to 4.1G, the other members of the protein

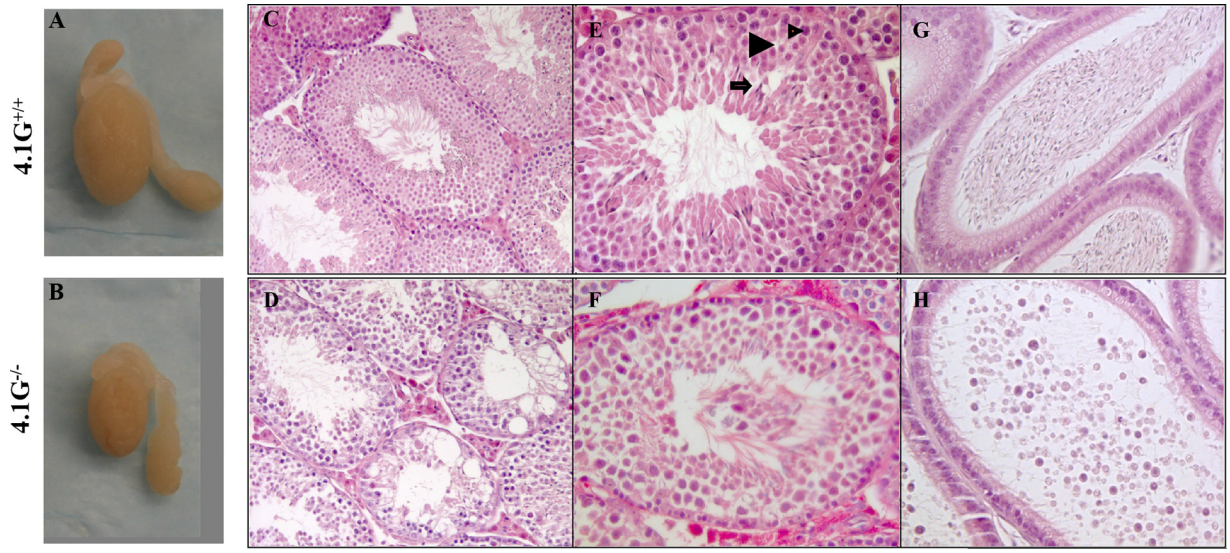

FIG. 3. Effects of 4.1G deficiency on testis. (A and B) Testis from 6-month-old mice. Note the significantly decreased size of $4.1G^{-/-}$ testis compared to normal testis at the same age. (C to F) Representative H&E-stained testis sections. Note the well-organized seminiferous epithelium (C [×20 magnification]) and normal spermatogenic features (E [×40 magnification]) in $4.1G^{+/+}$ testis. Small arrowhead, large arrowhead, and arrow indicate spermatogonia, round spermatids, and elongating spermatids, respectively. Note the atrophy, the decreased number of spermatogenic cells, the presence of vacuoles (D [×20 magnification]), and presence of sloughed cells in the lumen (F [×20 magnification]) in $4.1G^{-/-}$ testis. (G, H) Representative H&E-stained epididymis sections. Note the abundant mature spermatids in $4.1G^{+/+}$ (G [×20 magnification]) but not $4.1G^{-/-}$ (H [×20 magnification]) epididymis.

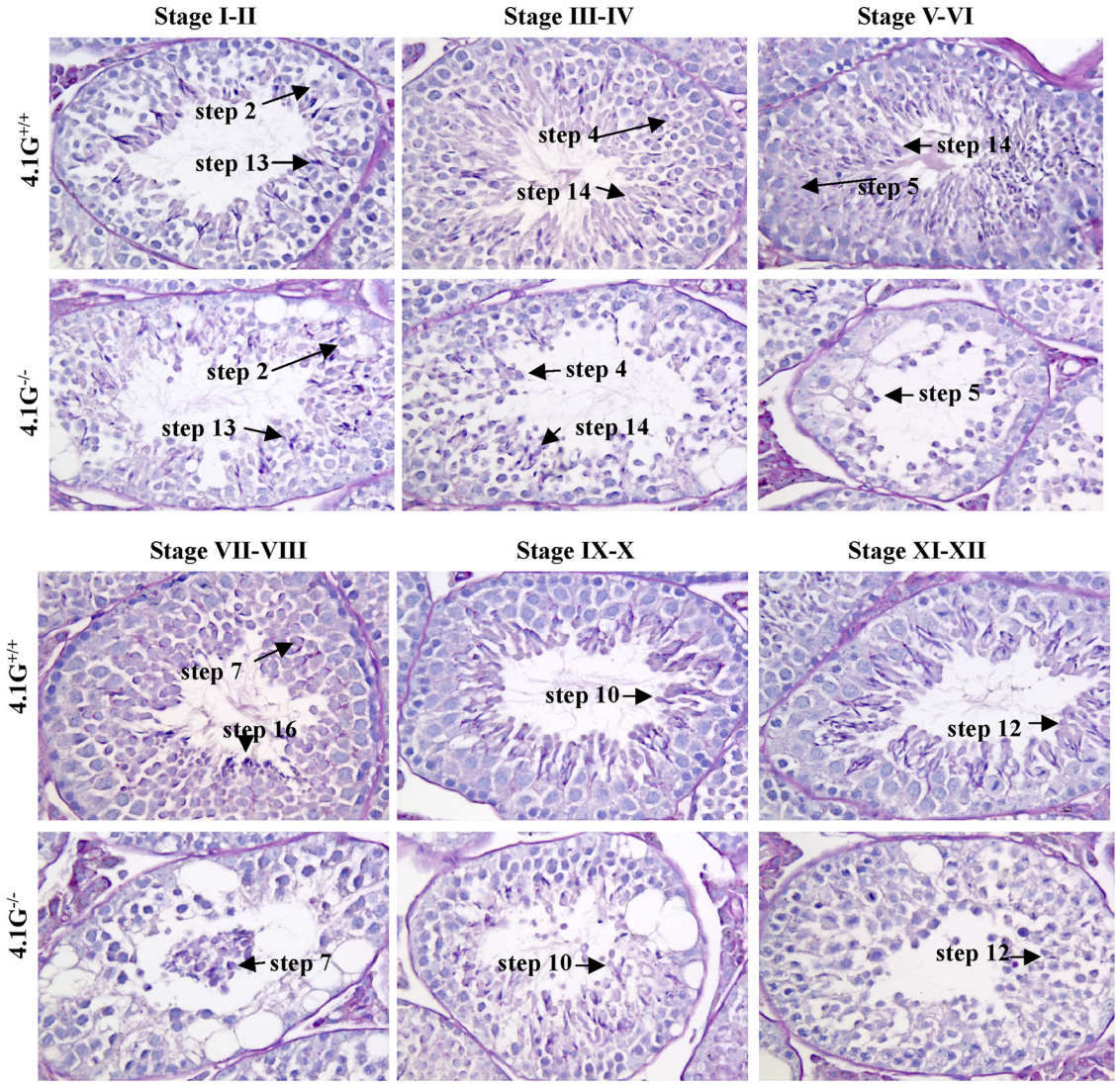

FIG. 4. Effect of 4.1G deficiency at different stages of spermatogenesis. Testis sections were stained with periodic acid-Schiff reagent. Representative pictures are shown. Note the atrophy, the decreased number of spermatogenic cells, the presence of vacuoles at all the stages, and the presence of sloughed premature spermatids near or in the lumen, especially around stage VII-VIII of $4.1G^{-/-}$ testis. Magnification, ×40.

4.1 family (4.1R, 4.1B, and 4.1N) are present in the testis, and their expression levels are unchanged in $4.1G^{-/-}$ testis (Fig. 1D).

Characterization of 4.1G isoforms in testis. Western blot analysis of testis tissue revealed the expression of three distinct isoforms. To further characterize these isoforms, we amplified the 4.1G transcripts from testis using a forward primer starting from the single initiation codon and a reverse primer from the end of the coding region. In agreement with Western blot analysis, RT-PCR generated three 4.1G transcripts from $4.1G^{+/+}$ testis that are not present in $4.1G^{-/-}$ testis (Fig. 2A). Analysis of the cDNA sequences revealed that none of the testis 4.1G isoforms contained exons 14 and 15. The transcript encoding the big isoform contains exons encoding all domains, namely the U1 region (exon 2), FERM domain (exons 4 to 12), U2 region (exon 13), SABD (exons 16 and 17), U3 region (exons 17C and an internally spliced 17D), and full-length CTD (exons 18 to 21). In contrast, the middle transcript (4.1G2) isoform lacks exons 16 and 17, which together encode the SABD. In addition, there is a splicing event after 315 bp in exon 17D, which joins directly to exon 19. The small transcript (4.1G3) lacks the SABD, the entire U3 region, and exon 18. This internal splicing or deletion of exons does not change the reading frame of the downstream encoded peptides. The exon composition of the three testis 4.1G isoforms is illustrated in Fig. 2B.

Deficiency of 4.1G in the B6-129 background is associated with male infertility. As mentioned earlier, the 4.1G knockout mouse was generated in a hybrid B6-129 background. Breeding of B6-129 heterozygous $4.1G^{+/-}$ mice yielded viable $4.1G^{-/-}$ homozygous mice at the expected Mendelian ratio. However, breeding experiments using homozygous mice revealed that despite normal vaginal plug formation in female mice, $4.1G^{-/-}$ male mice were unable to produce offspring. At autopsy, the

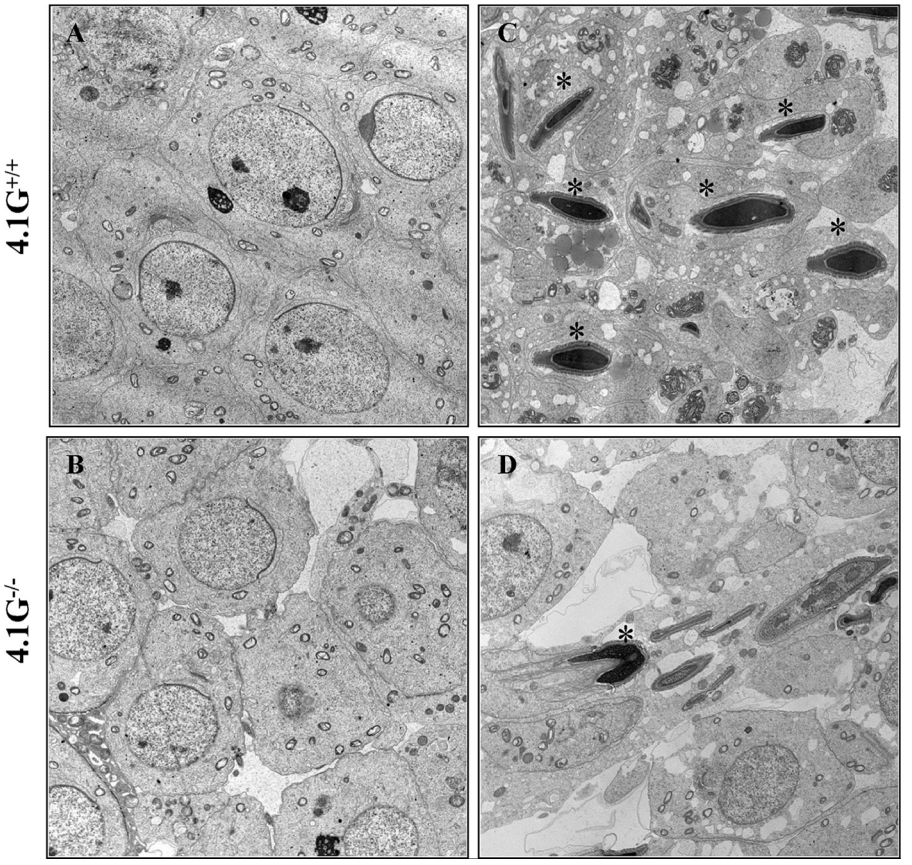

FIG. 5. Ultrastructural changes of $4.1G^{-/-}$ testis. (A and B) Representative images from the basal part of the seminiferous epithelium. In $4.1G^{+/+}$ seminiferous epithelium, the spermatogenic cells and Sertoli cells closely packed together (A). In the $4.1G^{-/-}$ testis, prominent extracellular spaces surrounding spermatogenic cells are present (B). (C and D) Representative images from the apical part of the seminiferous epithelium. Note the deformed nucleus of late-step spermatids in $4.1G^{-/-}$ testis seminiferous epithelium (D) compared to that of $4.1G^{+/+}$ testis (C). *, nucleus. Magnifications, ×5,400.

gross anatomy of $4.1G^{-/-}$ mice appeared normal except for the markedly reduced size and weight of the testes of $4.1G^{-/-}$ adult mice. Figures 3A and B show the representative images of $4.1G^{+/+}$ (Fig. 3A) and $4.1G^{-/-}$ (Fig. 3B) testes of 6-month-old mice. The weight of the $4.1G^{-/-}$ testis (82 ± 12 mg; $n = 5$) was around 54% of that of the $4.1G^{+/+}$ testis (152 ± 11 mg; $n = 5$; $P < 0.0001$, Student's t test). Surprisingly, however, when 4.1G knockout mice were bred for nine generations into the B6 background, male infertility was no longer a problem, and $4.1G^{-/-}$ male mice were able to produce offspring normally and had normal testis weight.

Histological changes of the testes and epididymides of $4.1G^{-/-}$ mice. Having demonstrated male infertility and markedly reduced testis size and weight, we then examined the histological changes of B6-129 $4.1G^{-/-}$ testes. Figures 3C and E reveal normal spermatogenesis in adult $4.1G^{+/+}$ mice, with the full spectrum of spermatogonia, spermatocytes, and spermatids at various stages of development. Large numbers of late-stage spermatids with elongating or elongated nuclei were present in the seminiferous epithelia. In contrast, profound changes were seen in the $4.1G^{-/-}$ adult testis. The seminiferous epithelium of $4.1G^{-/-}$ testis demonstrated atrophic changes with reduced thickness and a large number of vacuoles (Fig. 3D). Late-stage spermatids were seldom observed in $4.1G^{-/-}$ seminiferous epithelia, and immature or degenerated spermatogenic cells were seen in the lumens (Fig. 3F). The cell-cell contact appeared to be impaired in $4.1G^{-/-}$ seminiferous epithelium compared to that of $4.1G^{+/+}$ seminiferous epithelium. To assess the effects of the 4.1G deficiency on the interactions between spermatogenic cells and Sertoli cells through various stages of spermatogenesis, we performed PAS staining. As shown in Fig. 4, the above-described changes are observed at all stages of development. Furthermore, examination of the cauda epididymis demonstrated that whereas the $4.1G^{+/+}$ epididymis contained abundant mature sperm with elongated and condensed nuclei and thin tails (Fig. 3G), the $4.1G^{-/-}$ epididymis was filled with immature or degenerated spermatids with round nuclei and wide cytoplasmic compartments (Fig. 3H). Consistent with the normal fertility of $4.1G^{-/-}$ mice in the B6 background, no obvious pathological changes were observed in $4.1G^{-/-}$ testes from B6 mice (data not shown).

Ultrastructural changes of $4.1G^{-/-}$ testis. To further elucidate the pathological changes in B6-129 testis, electron microscopic examination was performed. Figures 5A and B are representative images taken from the basal region of $4.1G^{+/+}$ and $4.1G^{-/-}$ seminiferous epithelia, respectively. They revealed that in $4.1G^{+/+}$ seminiferous epithelium, the spermatogenic

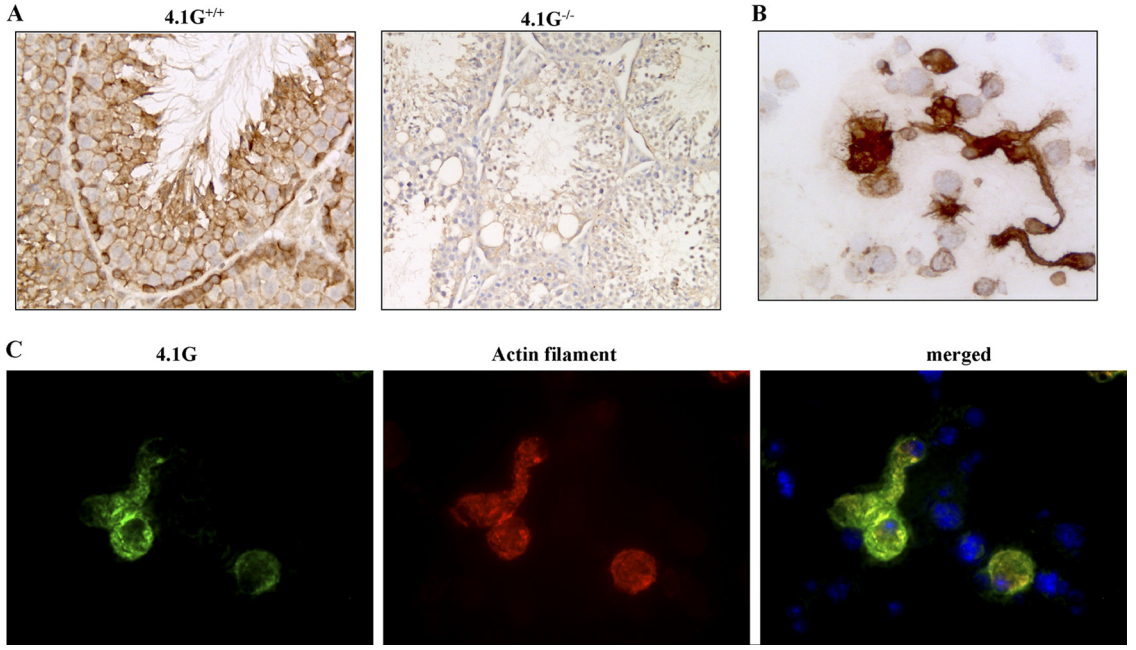

FIG. 6. Localization of 4.1G. (A) Immunostaining of 4.1G in testis tissues. Note that 4.1G is seen in the whole layer of seminiferous epithelium, predominantly on the membranes (left [×40 magnification]). No staining is observed on $4.1G^{-/-}$ testis (right [×20 magnification]). (B) Immunostaining of 4.1G in separated testis cells. Note the staining of 4.1G in a subset of cells with wide cytoplasm and multiple cell protrusions (×20 magnification). (C) Double staining of 4.1G and actin in separated testis cells. Note that the staining for both 4.1G and actin is seen only in cells with large cytoplasm.

and Sertoli cells were closely packed, and every spermatogenic cell was encircled by the well-developed slender protrusions from Sertoli cells (Fig. 5A). In contrast, in the $4.1G^{-/-}$ testis, prominent extracellular spaces surrounding spermatogenic cells were present, implying impaired cell-cell contact between spermatogenic cells and Sertoli cells (Fig. 5B). Figure 5C shows abundant late-stage spermatids in the lumen of $4.1G^{+/+}$ seminiferous epithelium. In contrast, in the lumen of $4.1G^{-/-}$ seminiferous epithelium, the late-stage spermatids were very rare and, when present, showed dramatic morphological defects, including double, deformed, and/or irregularly shaped nuclei, often with a large amount of residual body (Fig. 5D).

4.1G is expressed in Sertoli cells. To further explore the cellular and molecular basis for male infertility due to lack of 4.1G, we performed immunohistochemical staining to examine the location of 4.1G in testes. Figure 6A shows that 4.1G is expressed across the whole layer of the seminiferous epithelium and appears to be localized mainly along the membranes. The staining is specific, as it is negative in $4.1G^{-/-}$ testis. The testis is composed mainly of Sertoli cells and spermatogenic cells. Due to the intimate relationship between the two cell types, it is difficult to define whether 4.1G is expressed in Sertoli cells or spermatogenic cells or both at the tissue level. To address this, we performed immunohistochemistry staining on separated testis cell smears. Figure 6B reveals that 4.1G is expressed only on a subset of cells with large cytoplasm and multiple cell protrusions, which morphologically resemble Sertoli cells. The round spermatogenic cells are negative for 4.1G staining. The staining is also negative in $4.1G^{-/-}$ cells (data not shown). To further confirm the expression of 4.1G in Sertoli cells, we performed immunofluorescence staining for 4.1G and for actin filament, which is known to be abundantly present in Sertoli but not germ cells (26). Figure 6C shows that the staining of both 4.1G and actin filament is seen only in cells with large cytoplasm.

Association of 4.1G with NECL4. Both histologic analysis and electron microscopy (EM) examination demonstrated a defect in cell-cell contact between Sertoli cells and germ cells, which could be due to abnormal function of cadherin, nectin, or nectin-like (NECL) molecules secondary to the 4.1G deficiency (26). It has been shown that the cytoplasmic domain of NECL molecules contains a potential 4.1 binding motif identified previously in 4.1 binding proteins, such as glycophorin C (53). Expression of NECL2 (47) and NECL4 (50) has previously been identified in testis. Since NECL2 is expressed only on spermatogenic cells (47) while our data demonstrated that 4.1G is expressed in Sertoli cells, we surmised that NECL2 is unlikely to be the adhesive molecule affected by 4.1G deficiency. Instead, we hypothesized that a 4.1G-NECL4 association might be important for adhesive properties of Sertoli cells. To test this, we performed a series of experiments. Figure 7A shows the immunofluorescence staining of 4.1G and NECL4 and reveals the colocalization of 4.1G with NECL4 on seminiferous tubules. We performed coimmunoprecipitation assays to test for an interaction between 4.1G and NECL4 *in situ*. Figure 7B shows that NECL4 was coprecipitated by anti-4.1G antibody with 4.1G from $4.1G^{+/+}$ but not $4.1G^{-/-}$ testis. No coprecipitation was noted when the control antibody was used. Moreover, Fig. 7C shows that all three 4.1G isoforms coprecipitate with NECL4 from $4.1G^{+/+}$ but not in $4.1G^{-/-}$ testis. These results demonstrate the association between NECL4 and 4.1G *in situ*. We further confirmed the direct association

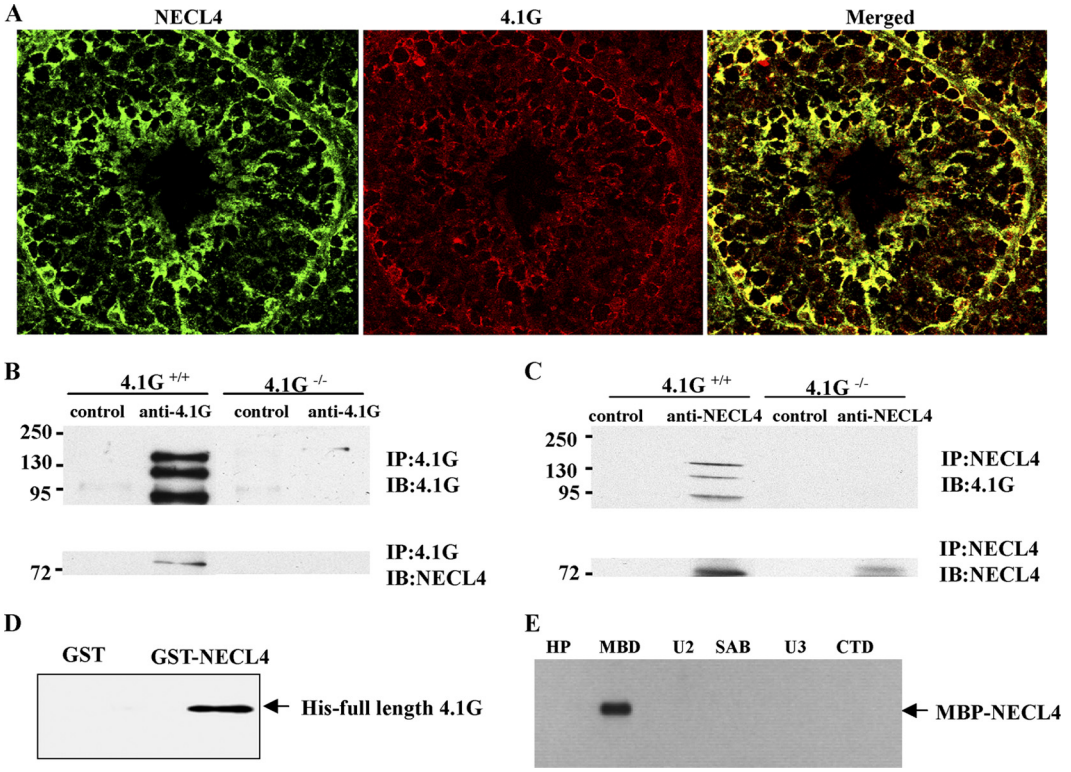

FIG. 7. Association of 4.1G with NECL4. (A) Costaining of 4.1G and NECL4. Frozen sections from $4.1G^{+/+}$ testis were costained with anti-NECL4 antibody (green) and anti-4.1G antibody (red). Merged image shows that 4.1G colocalizes with NECL4 in the testis tissue. (B) Coimmunoprecipitation of NECL4 with 4.1G. The lysate from $4.1G^{+/+}$ or $4.1G^{-/-}$ testis was immunoprecipitated by anti-4.1G or control rabbit IgG and detected by anti-4.1G antibody (top) or anti-NECL4 antibody (bottom), respectively. Note that NECL4 was brought down with 4.1G. (C) Coimmunoprecipitation of 4.1G with NECL4. The lysate from the $4.1G^{+/+}$ or $4.1G^{-/-}$ testis was immunoprecipitated by anti-NECL4 or control rabbit IgG and detected by anti-4.1G antibody (top) or anti-NECL4 antibody (bottom), respectively. Note that all three 4.1G isoforms were brought down with NECL4. (D) Direct binding of full-length 4.1G with NECL4. Recombinant His-tagged full-length 4.1G was incubated with the GST-tagged cytoplasmic domain of NECL4. Binding was detected by Western blotting, using anti-His antibody for detection. (E) Direct binding of the cytoplasmic domain of NECL4 to various domains of 4.1G. MBP-tagged cytoplasmic domain of NECL4 was incubated with GST-tagged 4.1G domains. Binding was assayed as described above, using anti-MBP antibody for detection.

between 4.1G and NECL4 using *in vitro* binding assays. Figure 7D shows that full-length 4.1G binds to the GST-tagged cytoplasmic domain of NECL4 but not to GST alone. We further showed that the 30-kDa membrane binding of 4.1G is responsible for the interaction (Fig. 7E).

Altered expression and localization of NECL4 in $4.1G^{-/-}$ testis. It is well established that members of the protein 4.1 family serve as adaptors linking transmembrane proteins to the cytoskeleton. For example, in red blood cells, lack of 4.1R leads to loss or decreased expression of several transmembrane proteins (37). Having shown the direct interaction between 4.1G and NECL4, we examined whether lack of 4.1G affects the expression and localization of NECL4. Western blot analysis revealed that NECL4 protein was significantly decreased in $4.1G^{-/-}$ testis (Fig. 8A). Decreased NECL4 was also observed in congenic B6 $4.1G^{-/-}$ testis. As a negative control, we showed that protein levels of cadherin-associated β-catenin were unaltered. To define the mechanism by which 4.1G loss leads to reductions in NECL4 protein levels, we performed real-time PCR. Figure 8B shows that there is little or no difference in the transcript levels of NECL4 between $4.1G^{+/+}$ and $4.1G^{-/-}$ testes, suggesting that the reduced level of NECL4 protein in $4.1G^{-/-}$ is not due to reduced transcription. Immunofluorescence staining of NECL4 revealed that NECL4 is localized on the membranes of $4.1G^{+/+}$ testis, while no clear membrane staining of NECL4 was observed in $4.1G^{-/-}$ testis (Fig. 8C). These findings imply that lack of 4.1G alters the extent of localization of NECL4 to the membrane, which in turn affects the intercellular adhesion between Sertoli cells and germ cells and contributes to the infertility of $4.1G^{-/-}$ male mice.

DISCUSSION

4.1G is a member of the protein 4.1 superfamily, which contains more than 40 members (40). Based on the wide distribution pattern of 4.1G transcripts, it has been long thought that 4.1G is generally expressed. However, our Western blotting revealed that out of the eight major organs/tissues examined, 4.1G is expressed in only three of them (brain, lung, and testis) but not in the other five (liver, prostate, small intestine, kidney, and skeletal muscle). This finding suggests that the concept that 4.1G is generally expressed needs to be reconsidered.

4.1G is abundantly expressed in brain, lung, and testis (maybe other tissues and cells); however, no overt defects other than male infertility are observed in 4.1G-deficient mice.

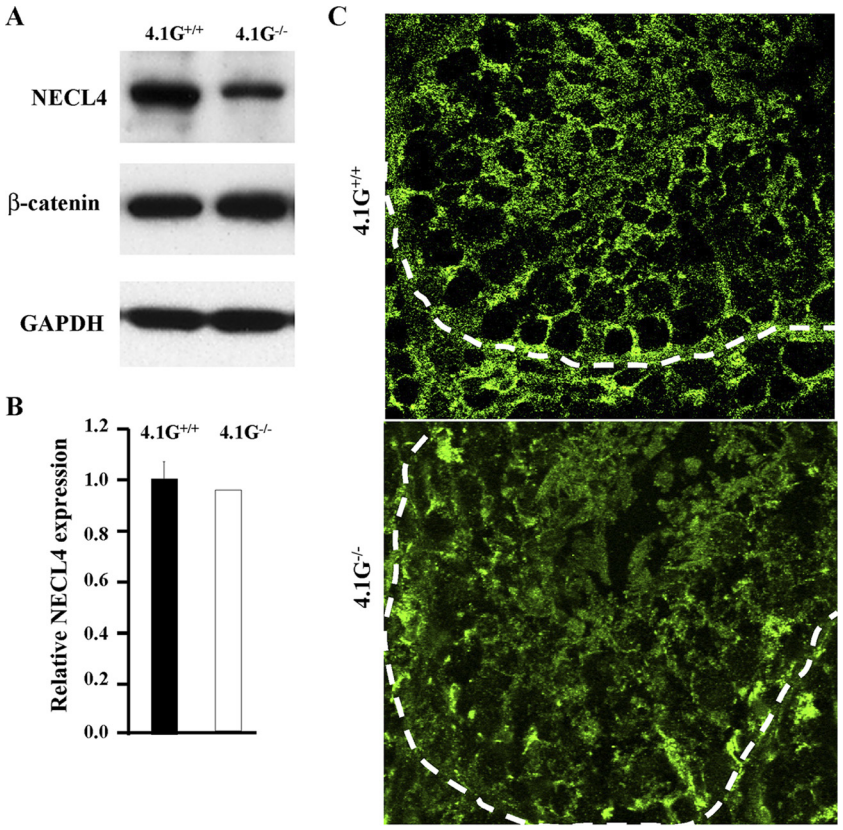

FIG. 8. Altered expression and localization of NECL4 in $4.1G^{-/-}$ testis. (A) Western blot analysis. Twenty micrograms of total protein from $4.1G^{+/+}$ or $4.1G^{-/-}$ testis was subjected to Western blot analysis, using the antibodies indicated. Note the significant reduction of NECL4 in $4.1G^{-/-}$ testis. (B) Real-time quantitative PCR (qPCR). The qPCR was performed as described in Materials and Methods. No significant difference was detected between $4.1G^{+/+}$ and $4.1G^{-/-}$ testes. (C) Immunofluorescence staining. Note the membrane staining of NECL4 in $4.1G^{+/+}$ but not $4.1G^{-/-}$ testis. The outlines of seminiferous tubules are indicated with dashed lines.

Since all protein 4.1 members are expressed in these tissues (our unpublished observations), it is possible that the function of 4.1G may be compensated by other members of the protein 4.1 family. Indeed, we have previously shown that all 4.1 family members are expressed in $CD4^+$ cells and that the expression of 4.1N is significantly upregulated in 4.1R-deficient $CD4^+$ T cells (17). We also found that all 4.1 family members are expressed in keratinocytes and that in 4.1R-deficient keratinocytes both 4.1N and 4.1G are upregulated (our unpublished observations). These findings suggest a compensatory mechanism among members of the protein 4.1 family. We are currently in the process of generating double or triple knockout mice, and it will be interesting in future studies to examine the phenotypic changes of these mice when they become available.

Although the present study clearly demonstrates an important role of 4.1G in spermatogenesis, it must be noted that this defect occurred only in B6-129 hybrid mice but not in congenic B6 mice, even though the NECL4 is decreased in both strains. Given the fact that genetic background has a profound effect on most phenotypes, our findings strongly suggest the presence of a gene modifier(s) which is associated with male infertility in strain 129/Sv. In the absence of specific crosses to map genetic modifiers (beyond the scope of this paper), it is not possible to say how and why reduction in NECL4 affects one but not the other background. In this context, it also should be noted that Terada et al. have recently shown that 4.1G knockout mice on a 129/S4-B6 mixed background were fertile (45). It has been reported that genetic variation among 129 substrains has important implications for targeted mutagenesis in mice (38, 39). Considering the fact that the phenotypical changes in 4.1G knockout testis are background dependent, it is highly possible that the differences between our findings and that of Terada et al. are due to different backgrounds. In fact, we also found that while B6 $4.1R^{-/-}$ mice are fertile, 129/Sv $4.1R^{-/-}$ mice are infertile (our unpublished observation).

It has been documented that members of the protein 4.1 family associate with a variety of transmembrane proteins and regulate the expression and/or the function of these proteins. For example, deficiency of 4.1R in erythrocytes leads to the altered expression of several transmembrane proteins (37). In $CD4^+$ T cells, 4.1R binds to the adapter protein LAT (linker of activation of T cells) and inhibits the phosphorylation of LAT (17). While 4.1G has been shown to bind metabotropic glutamate receptor (19), adenosine receptor (20), and parathyroid hormone receptor (36), 4.1N binds to IP3 receptor (23) and dopamine receptor (4). In the context of cell-cell contact and adhesion molecules, we have recently demonstrated that 4.1R is required for the formation of adherens junctions (AJs) in stomach epithelia through its direct interaction with beta-catenin (52). Denisenko-Nehrbass et al. have shown that 4.1B

plays an important role in linking the paranodal and juxtaparanodal adhesion complexes to the axonal cytoskeleton by interacting with Caspr and Caspr2 (12). The binding of members of the protein 4.1 family to other adhesion molecules has also been reported, such as the binding of 4.1B to the beta 8 integrin (24) and TSLC1 (51) and the binding of 4.1N to nectin-like 1 (53). Here, we show that 4.1G binds to the adhesion molecule NECL4 and that lack of 4.1G in testis resulted in the significantly decreased expression of NECL4 and the subsequent impairment of cell-cell contact between Sertoli cells and germ cells. Taken together, these findings imply a general role of protein 4.1 members in receptor and adhesion molecule-mediated functions.

Like other epithelia, the major cell-cell junctions in testis seminiferous epithelium are tight junctions (TJs) and adherens junctions. TJs are formed between Sertoli cells and are located at the basal compartment of the seminiferous epithelium membrane (which is in the opposite position compared with that of other epithelial cells, where the TJs occupy the most apical portion of the cell) (21). AJs are formed between Sertoli cells and germ cells or between Sertoli and Sertoli cells (22). While the AJs in other epithelial cells have been extensively studied (25), much less is known about the AJs in testis. Not only are AJs morphologically different from those in other epithelia (7), but the molecular components are also probably different. While it is well established that the formation of homotypic AJs in other epithelia is mediated largely by the homophilic interaction between Ca^{2+}-dependent cell adhesion molecules (also known as cadherins), the adhesive mechanism of heterotypic AJs in more complex tissues, such as seminiferous epithelium, remains to be clarified. The presence of cadherin/catenin-based AJs in testis has been controversial (2, 7, 11). Instead, there is evidence that the heterotypic *trans*-interaction between Ca^{2+}-independent adhesion molecules nectin-2 on Sertoli cells and nectin-3 on spermatids may play essential roles in coupling cell-cell adhesion in testis (27). The significantly impaired cell-cell contact between Sertoli cells and germ cells due to decreased NECL4 in $4.1G^{-/-}$ testis implies an important role of NECL4 in AJ formation in testis. Since nectins and NECLs preferentially mediate heterophilic interactions (41), it is possible that the heterotypic AJs between Sertoli and germ cells are mediated by nectins or NECLs rather than cadherins.

ACKNOWLEDGMENTS

We thank Phillipe D. Gascard for His-tagged recombinant full-length 4.1G and James Salzer for the GST-tagged cytoplasmic domain of NECL4 in pGEX-4T-3 vector and anti-NECL4 antibody.

This work was supported in part by NIH grants DK 26263, HL31579, HL088468, and DK32094.

REFERENCES

1. **Akama, T. O., et al.** 2002. Germ cell survival through carbohydrate-mediated interaction with Sertoli cells. Science **295:**124–127.
2. **Andersson, A. M., K. Edvardsen, and N. E. Skakkebaek.** 1994. Expression and localization of N- and E-cadherin in the human testis and epididymis. Int. J. Androl. **17:**174–180.
3. **Anway, M. D., J. Folmer, W. W. Wright, and B. R. Zirkin.** 2003. Isolation of Sertoli cells from adult rat testes: an approach to ex vivo studies of Sertoli cell function. Biol. Reprod. **68:**996–1002.
4. **Binda, A. V., N. Kabbani, R. Lin, and R. Levenson.** 2002. D2 and D3 dopamine receptor cell surface localization mediated by interaction with protein 4.1N. Mol. Pharmacol. **62:**507–513.
5. **Bustin, S. A.** 2010. Why the need for qPCR publication guidelines? The case for MIQE. Methods **50:**217–226.
6. **Bustin, S. A., et al.** 2009. The MIQE guidelines: minimum information for publication of quantitative real-time PCR experiments. Clin. Chem. **55:**611–622.
7. **Byers, S., R. Graham, H. N. Dai, and B. Hoxter.** 1991. Development of Sertoli cell junctional specializations and the distribution of the tight-junction-associated protein ZO-1 in the mouse testis. Am. J. Anat. **191:**35–47.
8. **Cheng, C. Y., and D. D. Mruk.** 2002. Cell junction dynamics in the testis: Sertoli-germ cell interactions and male contraceptive development. Physiol. Rev. **82:**825–874.
9. **Conboy, J., Y. W. Kan, S. B. Shohet, and N. Mohandas.** 1986. Molecular cloning of protein 4.1, a major structural element of the human erythrocyte membrane skeleton. Proc. Natl. Acad. Sci. U. S. A. **83:**9512–9516.
10. **Correas, I.** 1991. Characterization of isoforms of protein 4.1 present in the nucleus. Biochem. J. **279**(Pt. 2)**:**581–585.
11. **Cyr, D. G., O. W. Blaschuk, and B. Robaire.** 1992. Identification and developmental regulation of cadherin messenger ribonucleic acids in the rat testis. Endocrinology **131:**139–145.
12. **Denisenko-Nehrbass, N., et al.** 2003. Protein 4.1B associates with both Caspr/paranodin and Caspr2 at paranodes and juxtaparanodes of myelinated fibres. Eur. J. Neurosci. **17:**411–416.
13. **Gallup, J. M., and M. R. Ackermann.** 2008. The 'PREXCEL-Q method' for qPCR. Int. J. Biomed. Sci. **4:**273–293.
14. **Hellemans, J., G. Mortier, A. De Paepe, F. Speleman, and J. Vandesompele.** 2007. qBase relative quantification framework and software for management and automated analysis of real-time quantitative PCR data. Genome Biol. **8:**R19.
15. **Hellsten, E., et al.** 2002. Sertoli cell vacuolization and abnormal germ cell adhesion in mice deficient in an inositol polyphosphate 5-phosphatase. Biol. Reprod. **66:**1522–1530.
16. **Huang, S. C., R. Jagadeeswaran, E. S. Liu, and E. J. Benz, Jr.** 2004. Protein 4.1R, a microtubule-associated protein involved in microtubule aster assembly in mammalian mitotic extract. J. Biol. Chem. **279:**34595–34602.
17. **Kang, Q., et al.** 2009. Cytoskeletal protein 4.1R negatively regulates T-cell activation by inhibiting the phosphorylation of LAT. Blood **113:**6128–6137.
18. **Krauss, S. W., et al.** 2008. Downregulation of protein 4.1R, a mature centriole protein, disrupts centrosomes, alters cell cycle progression, and perturbs mitotic spindles and anaphase. Mol. Cell. Biol. **28:**2283–2294.
19. **Lu, D., H. Yan, T. Othman, and S. A. Rivkees.** 2004. Cytoskeletal protein 4.1G is a binding partner of the metabotropic glutamate receptor subtype 1 alpha. J. Neurosci. Res. **78:**49–55.
20. **Lu, D., et al.** 2004. Cytoskeletal protein 4.1G binds to the third intracellular loop of the A1 adenosine receptor and inhibits receptor action. Biochem. J. **377:**51–59.
21. **Lui, W. Y., D. Mruk, W. M. Lee, and C. Y. Cheng.** 2003. Sertoli cell tight junction dynamics: their regulation during spermatogenesis. Biol. Reprod. **68:**1087–1097.
22. **Lui, W. Y., D. D. Mruk, W. M. Lee, and C. Y. Cheng.** 2003. Adherens junction dynamics in the testis and spermatogenesis. J. Androl. **24:**1–14.
23. **Maximov, A., T. S. Tang, and I. Bezprozvanny.** 2003. Association of the type 1 inositol (1,4,5)-trisphosphate receptor with 4.1N protein in neurons. Mol. Cell. Neurosci. **22:**271–283.
24. **McCarty, J. H., A. A. Cook, and R. O. Hynes.** 2005. An interaction between {alpha}v{beta}8 integrin and band 4.1B via a highly conserved region of the band 4.1 C-terminal domain. Proc. Natl. Acad. Sci. U. S. A. **102:**13479–13483.
25. **Meng, W., and M. Takeichi.** 2009. Adherens junction: molecular architecture and regulation. Cold Spring Harb. Perspect. Biol. **1:**a002899.
26. **Mruk, D. D., and C. Y. Cheng.** 2004. Sertoli-Sertoli and Sertoli-germ cell interactions and their significance in germ cell movement in the seminiferous epithelium during spermatogenesis. Endocr. Rev. **25:**747–806.
27. **Mueller, S., T. A. Rosenquist, Y. Takai, R. A. Bronson, and E. Wimmer.** 2003. Loss of nectin-2 at Sertoli-spermatid junctions leads to male infertility and correlates with severe spermatozoan head and midpiece malformation, impaired binding to the zona pellucida, and oocyte penetration. Biol. Reprod. **69:**1330–1340.
28. **Nolan, T., R. E. Hands, and S. A. Bustin.** 2006. Quantification of mRNA using real-time RT-PCR. Nat. Protoc. **1:**1559–1582.
29. **Nolan, T., R. E. Hands, W. Ogunkolade, and S. A. Bustin.** 2006. SPUD: a quantitative PCR assay for the detection of inhibitors in nucleic acid preparations. Anal. Biochem. **351:**308–310.
30. **Parra, M., et al.** 2000. Molecular and functional characterization of protein 4.1B, a novel member of the protein 4.1 family with high level, focal expression in brain. J. Biol. Chem. **275:**3247–3255.
31. **Parra, M., et al.** 1998. Cloning and characterization of 4.1G (EPB41L2), a new member of the skeletal protein 4.1 (EPB41) gene family. Genomics **49:**298–306.
32. **Rice, P., I. Longden, and A. Bleasby.** 2000. EMBOSS: the European Molecular Biology Open Software suite. Trends Genet. **16:**276–277.
33. **Ruijter, J. M., et al.** 2009. Amplification efficiency: linking baseline and bias in the analysis of quantitative PCR data. Nucleic Acids Res. **37:**e45.

34. **Russell, L. D., R. A. Ettlin, A. P. Sinha Hikim, and E. J. Clegg.** 1990. Histological and histopathological evaluation of the testis, p. 1–52. Cache River Press, Clearwater, FL.
35. **Rutherford, K., et al.** 2000. Artemis: sequence visualization and annotation. Bioinformatics **16:**944–945.
36. **Saito, M., et al.** 2005. Increase in cell-surface localization of parathyroid hormone receptor by cytoskeletal protein 4.1G. Biochem. J. **392:**75–81.
37. **Salomao, M., et al.** 2008. Protein 4.1R-dependent multiprotein complex: new insights into the structural organization of the red blood cell membrane. Proc. Natl. Acad. Sci. U. S. A. **105:**8026–8031.
38. **Sechler, J. M., J. C. Yip, and A. S. Rosenberg.** 1997. Genetic variation among 129 substrains: practical consequences. J. Immunol. **159:**5766–5768.
39. **Simpson, E. M., et al.** 1997. Genetic variation among 129 substrains and its importance for targeted mutagenesis in mice. Nat. Genet. **16:**19–27.
40. **Sun, C. X., V. A. Robb, and D. H. Gutmann.** 2002. Protein 4.1 tumor suppressors: getting a FERM grip on growth regulation. J. Cell Sci. **115:** 3991–4000.
41. **Takai, Y., J. Miyoshi, W. Ikeda, and H. Ogita.** 2008. Nectins and nectin-like molecules: roles in contact inhibition of cell movement and proliferation. Nat. Rev. Mol. Cell Biol. **9:**603–615.
42. **Taylor-Harris, P. M., et al.** 2005. Expression of human membrane skeleton protein genes for protein 4.1 and betaIISigma2-spectrin assayed by real-time RT-PCR. Cell. Mol. Biol. Lett. **10:**135–149.
43. **Taylor-Harris, P. M., et al.** 2005. Cardiac muscle cell cytoskeletal protein 4.1: analysis of transcripts and subcellular location—relevance to membrane integrity, microstructure, and possible role in heart failure. Mamm. Genome **16:**137–151.
44. **Tchernia, G., N. Mohandas, and S. Shohet.** 1981. Deficiency of skeletal membrane protein band 4.1 in homozygous hereditary elliptocytosis. Implications for erythrocyte membrane stability. J. Clin. Invest. **68:**454–460.
45. **Terada, N., et al.** 2010. Involvement of a membrane skeletal protein, 4.1G, for Sertoli/germ cell interaction. Reproduction **139:**883–892.
46. **Terada, N., et al.** 2005. Immunohistochemical study of a membrane skeletal molecule, protein 4.1G, in mouse seminiferous tubules. Histochem. Cell Biol. **124:**303–311.
47. **Wakayama, T., et al.** 2003. Expression and functional characterization of the adhesion molecule spermatogenic immunoglobulin superfamily in the mouse testis. Biol. Reprod. **68:**1755–1763.
48. **Walensky, L. D., et al.** 1999. A novel neuron-enriched homolog of the erythrocyte membrane cytoskeletal protein 4.1. J. Neurosci. **19:**6457–6467.
49. **Wang, H., et al.** 2010. Comprehensive characterization of expression patterns of protein 4.1 family members in mouse adrenal gland: implications for functions. Histochem. Cell Biol. **134:**411–420.
50. **Williams, Y. N., et al.** 2006. Cell adhesion and prostate tumor-suppressor activity of TSLL2/IGSF4C, an immunoglobulin superfamily molecule homologous to TSLC1/IGSF4. Oncogene **25:**1446–1453.
51. **Yageta, M., et al.** 2002. Direct association of TSLC1 and DAL-1, two distinct tumor suppressor proteins in lung cancer. Cancer Res. **62:**5129–5133.
52. **Yang, S., X. Guo, G. Debnath, N. Mohandas, and X. An.** 2009. Protein 4.1R links E-cadherin/beta-catenin complex to the cytoskeleton through its direct interaction with beta-catenin and modulates adherens junction integrity. Biochim. Biophys. Acta **1788:**1458–1465.
53. **Zhou, Y., et al.** 2005. Nectin-like molecule 1 is a protein 4.1N associated protein and recruits protein 4.1N from cytoplasm to the plasma membrane. Biochim. Biophys. Acta **1669:**142–154.